Published in final edited form as:
J Mol Biol. 2014 January 23; 426(2): 332–346. doi:10.1016/j.jmb.2013.09.037.

Novel Interaction of Ornithine Decarboxylase with Sepiapterin Reductase Regulates Neuroblastoma Cell Proliferation

Ingo Lange[1], **Dirk Geerts**[3], **David J. Feith**[4,+], **Gabor Mocz**[5,+], **Jan Koster**[6], and **André S. Bachmann**[1,2,*]

[1]Department of Pharmaceutical Sciences , The Daniel K. Inouye College of Pharmacy, University of Hawaii at Hilo, Hilo, HI 96720, USA [2]Department of Cell and Molecular Biology, John A. Burns School of Medicine, University of Hawaii at Manoa, Honolulu, HI 96813, USA [3]Department of Pediatric Oncology/Hematology, Sophia Children's Hospital, Erasmus University Medical Center, 3015 GE Rotterdam, The Netherlands [4]Department of Cellular and Molecular Physiology, Pennsylvania State University College of Medicine, Hershey, Pennsylvania, PA 17033, USA [5]Pacific Biosciences Research Center, University of Hawaii at Manoa, Honolulu, HI 96822, USA [6]Department of Oncogenomics, Academic Medical Center, University of Amsterdam, 1105 AZ Amsterdam, The Netherlands

Abstract

Ornithine decarboxylase (ODC) is the sentinel enzyme in polyamine biosynthesis. Both ODC and polyamines regulate cell division, proliferation, and apoptosis. Sepiapterin reductase (SPR) catalyzes the last step in the biosynthesis of tetrahydrobiopterin (BH_4), an essential cofactor of nitric oxide synthase (NOS), and has been implicated in neurological diseases but not yet in cancer. In this study, we present compelling evidence that native ODC and SPR physically interact, and we defined the individual amino acid residues involved in both enzymes using *in silico* protein-protein docking simulations. The resulting heterocomplex is a surprisingly compact structure, featuring two energetically and structurally equivalent binding modes both in monomer and dimer conformations. The novel interaction between ODC and SPR proteins was confirmed under physiological conditions by co-immunoprecipitation and co-localization in neuroblastoma (NB) cells. Importantly, we showed that siRNA-mediated knock-down of SPR expression

*Correspondence to André S. Bachmann, Department of Pharmaceutical Sciences, The Daniel K. Inouye College of Pharmacy, University of Hawaii at Hilo, 34 Rainbow Drive, Hilo, HI 96720, USA. Tel: +808-933-2807; Fax: +808-933-2974; andre@hawaii.edu.
+Equal Contribution

Author Contributions

A.S.B. initiated this work and wrote the R01 grant proposal which included the design of experiments; I.L., D.J.F., G.M., D.G., and J.K. performed experiments; A.S.B., I.L., D.G., D.J.F., G.M., and J.K. analyzed data; and A.S.B., I.L., and D.G. wrote the paper. All authors edited the final manuscript.

Supplementary Data

Supplementary data to this article can be found online.

significantly reduced endogenous ODC enzyme activity in NB cells, thus demonstrating the biological relevance of the ODC-SPR interaction. Finally, in a cohort of 88 human NB tumors we found that high SPR mRNA expression correlated significantly with poor survival prognosis using a Kaplan-Meier analysis (Logrank test $P = 5 \cdot 10^{-4}$), suggesting an oncogenic role for SPR in NB tumorigenesis. In conclusion, we showed that ODC binds SPR and thus propose a new concept in which two well-characterized biochemical pathways converge via the interaction of two enzymes. We identified SPR as a novel regulator of ODC enzyme activity, and based on clinical evidence present a model in which SPR drives ODC-mediated malignant progression in NB.

Introduction

Ornithine decarboxylase (ODC; EC 4.1.1.17) catalyzes the conversion of ornithine to putrescine, a precursor in the synthesis of the polyamines spermidine and spermine. ODC has transforming and oncogenic properties [1; 2], and elevated ODC and polyamine levels are linked to cell proliferation and cancer development [3; 4]. ODC is a direct target of the transcription factor Myc and is required for Myc-induced lymphoma development [5]. Research investigating the role of ODC and ODC-associated proteins as oncogenic factors in neuroblastoma (NB), a pediatric malignancy that arises in neural crest-derived cells of the sympathetic nervous system, has gained significant momentum [6; 7; 8; 9; 10; 11; 12; 13; 14; 15; 16; 17]. Evidence exists that ODC is a direct transcriptional target of the Myc-related MYCN transcription factor [18; 19], and it is therefore not surprising that the role of ODC and ODC-associated proteins is especially clear in the aggressive NB tumors that show amplification of the MYCN gene [20; 21; 22].

It has been well documented that antizyme (OAZ) proteins are negative regulators of cellular polyamine content and OAZ protein levels are controlled via a unique feedback mechanism that involves a +1 frame-shift during translation, induced by high cellular polyamine levels [23]. So far, OAZs are the only proteins described that physically interact with ODC, thereby regulating its enzymatic activity [24; 25; 26]. Under physiological conditions, ODC functions as a homodimer which generates two active sites at the dimer interface that contain residues contributed by each subunit [27]. ODC cycles between monomeric and dimeric forms and ODC activity resides exclusively in the dimeric form. A catalytically dead ODC protein can exhibit dominant-negative properties [28]. In addition, OAZ binding to ODC monomer leads to its inactivation and ubiquitin-independent proteasomal degradation [29]. The predominant OAZ family member is antizyme 1 (OAZ1); OAZ2 is usually expressed at significantly lower concentrations and OAZ3 expression is restricted to the testis [30; 31]. Two antizyme inhibitors, AZIN1 and AZIN2 further contribute to the regulation of ODC enzyme activity, testament to the level of complexity that governs cellular ODC expression in maintaining polyamine homeostasis. Both AZINs are strikingly similar to ODC but completely lack decarboxylase activity due to critical amino acid substitutions [32]. Of note, AZINs bind to OAZ with greater affinity than ODC, leading to a natural competition and liberation of ODC from the inactive ODC-OAZ heterodimer complex [33; 34; 35]. An edited form of AZIN1 with a greater affinity for OAZ than wild-type AZIN1 was recently described in hepatocellular carcinoma and the resultant higher AZIN1

protein stability further promotes cell proliferation through the neutralization of OAZ-mediated degradation of ODC and cyclin D1[36].

In the present study, we report the discovery of a novel interaction between ODC and sepiapterin reductase (SPR; EC 1.1.1.153), an enzyme that converts 6-pyruvoyl tetrahydropterin to tetrahydrobiopterin (BH_4) [37]. BH_4 is an essential cofactor of nitric oxide synthase (NOS), which converts arginine to nitric oxide (NO) and citrulline in the urea cycle [38]. Arginine is the precursor to ornithine, the ODC substrate for polyamine production, thus proposing a tantalizing concept, in which two well-characterized biochemical pathways with distinct functions converge via the interaction of two enzymes, ODC and SPR. While the SPR gene has been implicated in Parkinson's disease and its deficiency is associated with neurotransmitter disorders and cerebral palsy [39; 40], the role of SPR in cancer has never been studied. Our discovery that SPR is a new regulator of ODC activity led us to investigate its role in NB, where ODC has a clear oncogenic role and we now also present the first clinical evidence suggesting an oncogenic role for SPR in NB tumorigenesis.

Results

Molecular interaction prediction of ODC and SPR *in silico*

The physical interaction of ODC with SPR was previously identified at a high confidence interval using a yeast two-hybrid genome wide screening approach [41]. To verify the validity of this novel protein-protein association, the crystallographic structures of human ODC (1D7K) and human SPR (1Z6Z) were used for *in silico* docking simulations (Fig. 1).

It has been well documented that the biological unit for both ODC and SPR proteins is a homodimer [42; 43; 44]. We therefore restricted the simulations to solutions between dimers and also modeled the interaction between individual monomers. In crystals, SPR exists as a hexamer that contains three biological units. Two docking approaches were used in tandem to predict the amino acid residues that make up the interface between the two proteins, ODA [45] and GRAMM-X [46], (see Materials and Methods for approach details). The ODA methodology identified the basic surface elements involved in the dimerization of ODC, as well as in the dimerization and subsequent trimerization of SPR. It also predicted two surface area patches on both proteins that may play a role in heterocomplex formation. These areas were also highly ranked in GRAMM-X predictions. GRAMM-X returned a list of potential binding sites for heterocomplexes of dimers and their respective individual monomers. Every prediction from ODA and GRAMM-X was examined for surface patches found in both monomers and dimers. Binding sites unique to one but not both prediction methods or exclusive to monomer-monomer or dimer-dimer interactions were rejected. This filtering reduced the number of putative sites to only two areas.

Fig. 1a and Fig. 1b show the docking of individual monomers. The chains appear to interact at a depression between the TIM-like α/β barrel and the C-terminal sheet domain of ODC. The two SPR chains bind in the same area but with opposite orientation. Fig. 1c and Fig. 1d illustrate the characteristics of the dimer-dimer heterocomplex. The distance between the binding sites in the ODC dimer precisely matches the separation of the two inverted chains in the SPR dimer, thus determining and dictating their modes of interaction. The dimers

associate essentially at the same docking location as the monomers. The binding energy is almost equal for A and B chains while monomer-monomer docking favors B chain to B chain associations and gives higher rankings. In either case, the monomers and dimer pairs form a tightly bound stiff association with each configuration strongly supporting the validity of this *in silico* interaction model. The resulting quaternary structure probably hinders ligand access to the catalytic site of ODC, thereby affecting its enzymatic functions. Fig. 1e and Fig. 1f provide a close-up view of the respective docking areas. At an intermolecular distance cutoff of 7 Å, the binding site in the ODC-A chain is comprised of S160-K161, A162, G201, T203-E206, E242-V244, K245, K247, E250, H335, K337, and R369. Residues that are invariant to the order of proteins in the simulations are underlined. The corresponding residues in the SPR-A chain are K137, D141, P143-L145, R147, L183, E185, P186-N187, R189, D245-E246, and K248. In the analogous region of the ODC-B chain, A162-V163, C164-R165, G201, T203, I329, H333, H335, K337-P338, L363, V367, E368-R369 make up the interface. The counterpart residues on SPR B chain are predicted to be S105, Q204, E208-T209, D214-M215, K217-G218, Q220-E221, K223-A224, K225, and K227. Remarkably, a considerable number of polar and charged residues are found to contribute to the interface.

ODC residues A162, G201, T203, H335, K337, and R369 are common to both modes of binding and are marked by red in Fig. 1e and Fig. 1f, and highlighted in the primary amino acid sequence of ODC (Supplemental Fig. 1). The unique residues are specific for a particular orientation of the SPR monomers. These residues are K161, K245, and K247 in the ODC-A chain and V163, I329, V367, and E368 in the ODC-B chain, respectively. The two binding modes appear to be a direct result of the specific geometric structure of the dimer pairs. The separation distances for pairs of component chains in the two dimers are very similar and the dimer pairs display shape complementarity on their monomer constituents allowing them to lock together as a unit. However, one may argue that the interaction of monomers or dimers results in conformational changes that affect the two binding modes. Semi-rigid docking showed no clear indication for this possibility. The so-called soft-belt sites (*i.e.* into which atoms from the docking partner can penetrate in the simulations) were found to be slightly different but in essence identical to the binding sites depicted on Fig. 1. The sites were close, although not strictly the same in the monomers and dimers because the chains were somewhat rotated in the dimer in comparison with the monomers. However, this does not necessarily lead to larger conformational changes or longer range alterations between parts of the molecule.

It should be noted that due to symmetries of the two homodimers, antiparallel complexes (SPR-A chain to ODC-B chain and SPR-B chain to ODC-A chain) are equally possible; a 180 degree rotation along the dimer symmetry axis results in identical fits that are indistinguishable from the parallel (SPR-A chain to ODC-A chain and SPR-B chain to ODC-B chain) assemblies shown in Fig. 1. In summary, our *in silico* data clearly support the yeast two-hybrid findings reported by Giot *et al.* [41] and provide strong evidence that SPR is a novel ODC binding partner.

Co-localization and physical interaction of endogenous ODC and SPR

To confirm this novel interaction we first performed epifluorescence and laser-scanning confocal microscope experiments (Fig. 2a and Fig. 2b). We visualized endogenous ODC- and SPR-proteins using the Operetta High-Content Cell Imaging System in a 96-well format at 20X magnification, with DAPI (blue) as a nuclear counter stain (Fig. 2a, panels I-IV). While these epifluorescence images do not directly prove co-localization, they provided first evidence that ODC and SPR are located at similar sub-cellular sites. The co-localization between endogenous ODC and SPR proteins was subsequently verified using a laser-scanning confocal microscope, clearly showing that ODC and SPR co-localize (Fig. 2b). In accordance with previous reports, both ODC [47] and SPR (proteinatlas.org) primarily reside in the cytoplasm. In the MYCN2 NB cell line used in this study, ODC and SPR resided in punctuate sites within the cytoplasm.

To establish that ODC and SPR physically interact under physiologically-relevant conditions, we immunoprecipitated endogenous ODC-SPR complexes from MYCN2 NB cells and analyzed immunoprecipitates and cell lysates by Western blot, using ODC- and SPR-specific antibodies (Fig. 2c). Immunoprecipitation of ODC using ODC-specific agarose-conjugated antibodies led to the detection of two strong bands in close proximity at around the indicated molecular weight for ODC at 51 kDa and endogenous SPR clearly co-immunoprecipitated (lane 2), thus suggesting the physical interaction between endogenous ODC and SPR. A cell lysate with over-expressed SPR protein was loaded as control for protein size comparison (lane 1). To further evaluate the specificity of our reaction we performed the same ODC immunoprecipitation in the presence of ODC blocking peptide (BP). The BP prevented the binding of endogenous ODC to the agarose-conjugated antibody and efficiently inhibited the immunoprecipitation of ODC and associated SPR, as shown by the fact that both signals for ODC and SPR were clearly suppressed (lane 3). Additional controls included the analysis of cell lysates before and after immunoprecipitation (lanes 4–6). As anticipated, ODC and SPR protein levels were lower in cell lysates after immunoprecipitation because they were immunoprecipitated out by binding to ODC-specific agarose conjugated antibodies. The use of the ODC BP antagonized this reaction, as indicated with stronger bands for ODC and SPR. As an additional control, the immunoprecipitation of p27 was performed and then probed with ODC- and SPR-specific antibodies. ODC and SPR were not immunoprecipitated and remained in the cell lysates (Supplemental Fig. 2). In summary, our results strongly demonstrate that ODC and SPR physically associate under physiologically relevant conditions and at native cellular enzyme quantities/concentrations.

SPR contributes to NB cell proliferation

The role of SPR in cancer cell proliferation has not yet been studied. We therefore decided to assess if SPR alters cell proliferation in NB cells. SPR expression can readily be down-regulated using SPR-specific siRNA (mean signal 19.0% of control group, sdev= 8.6, n=8) in comparison to cells treated with non-targeting siRNA or control cells in the absence of siRNA (Fig. 3a) and the effect of SPR downregulation in NB cells was measured 72 hours later. Clearly, the knockdown of SPR led to a significant and consistent decrease in cellular proliferation (Fig. 3b). Similarly, ODC knock-down with ODC-specific siRNA (Mean signal

57.3% of control group, sdev= 3.8, n=3; Fig.3c) resulted in a comparable reduction of cellular proliferation (Fig. 3d). Of note, the reduction of cell proliferation by transient SPR knock-down as well as by stable ODC knock-down was independently confirmed in the non-cancerous human embryonic kidney 293 (HEK293) cell line (Supplemental Fig. 3). Our results propose that SPR plays a role in decreasing the proliferation of cancer cells and suggest that SPR binding and regulation of ODC may be a general mechanism that is also relevant in non-cancerous cell types.

SPR regulates ODC enzyme activity in NB cells

The metabolic activity of ODC is a crucial component in cell proliferation [48]. As demonstrated above, our data not only suggest that ODC and SPR directly interact at physiologically relevant protein levels, but also regulate cell proliferation. We were therefore curious to find out if altering SPR protein levels would have a direct impact on the enzymatic function of ODC. We tested this hypothesis by measuring the enzyme activity of endogenous ODC in lysates of NB cells in which SPR expression was down-regulated by siRNA. Controls included cells transfected with scrambled siRNA and mock-transfected cells. For SPR down-regulation, we used 2 different electroporation protocols, changing the voltage amplitude but not the pulse duration, leading to a slightly stronger knock-down in program II (P-II) (mean signal 13.1% of control group, sdev= 5.7, n=5) than in program I (P-I) (mean signal 22.6% of control group, sdev= 8.4, n=3) (Fig. 4a) (see methods section for details). Interestingly, the intensity of knock-down of SPR was directly proportional to the reduction of cell proliferation. Knock-down of SPR using P-I led to a significant reduction in proliferation ($P = 1.5 \cdot 10^{-3}$) which was further intensified ($P = 3.0 \cdot 10^{-4}$) by P-II (Fig. 4b and Fig. 4c). Remarkably, the knock-down of SPR was directly correlated with ODC enzymatic activity because cells with suppressed SPR expression showed a significant decrease of ~60% and 70% in enzymatic ODC activity ($P = 0.043$ and $P = 0.016$ in Fig. 4d and Fig. 4e), respectively. These data suggest that the presence of SPR is important to maintain ODC enzymatic activity, presumably via ODC-SPR interaction which controls polyamine-driven cellular proliferation through an unknown mechanism, possibly by out-competing the only ODC regulator described in literature so far, OAZ.

Clinical relevance of SPR in NB

We and others previously revealed the importance of ODC and regulation in several cancer forms including NB [6; 8; 13; 16; 49; 50]. We also showed that ODC and OAZ2 predict aggressive behavior in NBs with and without MYCN amplification [8]. In this study, we wanted to assess a potential role for SPR in NB, as suggested by its importance for NB cell survival *in vitro* as demonstrated above. We therefore examined whether SPR gene expression correlated with NB patient survival in a previously described cohort of 88 NB tumors. For these 88 tumors, extensive genetic and clinical descriptions were available from the patient files at the Academic Medical Center – University of Amsterdam, the Netherlands. Genome-wide Affymetrix U133Plus2.0 mRNA profiles were generated for these tumors, allowing insight into the clinical significance of interesting genes [8; 51; 52; 53; 54].

Kaplan-Meier analysis using SPR mRNA levels in these 88 tumor samples showed that high SPR expression is correlated with poor prognosis. In a follow-up of 216 months, overall survival of patients with low SPR tumor expression (n=51) remained around 80%, while that of patients with high SPR tumor expression (n=37) quickly fell to below 50%. This difference represents a *P* value of 0.036 (Logrank test). Also for median or average SPR cut-off values, significant correlations were found (data not shown). For all three groupings, a significant association between high SPR expression and patient death was found (Fig. 5a, see also legend). Interestingly, high SPR expression was still predictive of poor outcome in the 72 NB tumor set which is stratified for tumors without MYCN amplification (data not shown), suggesting that SPR is also a prognostic marker independent of MYCN.

Since ODC expression is essential for NB proliferation and survival, and SPR binding influences ODC enzyme activity, we questioned whether ODC and SPR expression was in any way linked. Fig. 5b shows a visual representation of ODC and SPR mRNA expression measured with Affymetrix profiling for each of the 88 tumors in the set. A clear positive correlation was observed [r = 0.289, $P = 6.2 \cdot 10^{-3}$ (Pearson)]. Both ODC and SPR mRNA expressions were highest in tumors that represent high patient age, high tumor stage, and MYCN gene amplification, all indicators of poor survival. In further support to the cooperative action of ODC and SPR demonstrated above, this suggests that aggressive NB tumors benefit from, and might select for, a combined high expression of both enzymes.

Discussion

Polyamines are well-studied molecules that are necessary for normal cell processes including embryonic development and an over-abundance of intracellular polyamines may contribute to uncontrolled cell proliferation, as observed in NB [3]. Polyamines play a central role in multiple signaling pathways and regulate distinct cellular functions[3; 4; 55]. Due to the positive charges distributed across the polyamine molecule, they are able to bind to DNA, RNA and protein, and regulate fundamental cellular processes by influencing DNA-synthesis/replication, RNA transcription /translation and protein function. However, the precise mechanisms by which polyamine levels are regulated are not yet fully understood. ODC is the first and rate-limiting enzyme of polyamine biosynthesis and, as such, has become a prime target for therapeutic intervention of NB. The suicide inhibitor alpha-difluoromethylornithine (DFMO), which is used in the treatment of African Sleeping Sickness (trypanosomiasis), was recently re-introduced in a phase I study in combination with etoposide for the treatment of relapsed/refractory NB [6; 16; 56] after the completion of a series of pre-clinical studies [9; 10; 11; 12; 13]. A phase II study to assess DFMO for chemoprevention potential in NB patients in remission with high risk for relapse is currently underway at several U.S. children's hospitals in affiliation with the Neuroblastoma and Medulloblastoma Research Consortium (NMTRC).

The goal of this study was to identify novel components in the cellular signaling network that might contribute to ODC regulation. Given the importance of ODC in MYCN-driven tumors like NB [8; 12] this study was primarily conducted in NB cells and tumors. So far, OAZs have been the only proteins known to physically interact with ODC. They are major regulators of ODC and inhibit ODC activity by complex formation as well as by facilitating

the proteasomal degradation of ODC. AZINs are positive regulators of ODC and bind with about 6-fold higher affinity to OAZs, thereby occluding them from binding to ODC. This competing relationship between ODC-OAZ and OAZ-AZIN is a remarkable adaptation to fine-tune the regulation of ODC activity, and thereby polyamine homeostasis. We here present strong evidence that the well-characterized ODC-OAZ-AZIN trio is further joined by a new player, SPR. Our data show that the polyamine biosynthesis regulating ODC enzyme interacts with SPR, an enzyme that regulates the synthesis of NOS cofactor BH_4, therefore suggesting that two well-described metabolic pathways converge and cross-communicate (Fig.6a). The validity of this novel interaction was also confirmed by using x-ray crystallographic data for ODC and SPR and advanced computational modeling to predict individual amino acid residues that engage in heterodimerization. Our data further revealed that ODC requires the presence of SPR because reduced SPR levels significantly decreased ODC enzyme activity, resulting in reduced proliferation rates (Fig. 4d, Fig. 4e and Fig. 6b). Importantly, these activity alterations were observed at native, physiologically relevant (*i.e.*, not over-expressed) enzyme concentrations, thus confirming the biological significance of this novel protein-protein interaction between ODC and SPR. Whether or not ODC inhibition or ODC downregulation affects NO production and/or alters SPR enzyme activity remains to be determined.

Relatively little is known about the *SPR* gene, which is located on chromosome 2 (cytogenetic location 2p14-p12). Most information to date relates to its possible role in the pathogenesis of Parkinson's disease. *SPR* is a candidate gene for the PARK3 locus and SPR null-mutant mice exhibit Parkinsonian features [40]. Importantly, a homozygous frame shift mutation of SPR was recently identified, causing Parkinsonism with onset in childhood [57]. SPR deficiency is inherited in an autosomal recessive fashion and the SPR phenotype is characterized by core Parkinsonian features including axial hypotonia, motor and language/developmental delays, dystonia, impaired motor skills and treatable mimics of cerebral palsy [39]. Of note, the polyamine pathway is implicated in the pathogenesis of Parkinson's disease [58] and SPR might be a contributing factor through its interaction with ODC and regulation of polyamines. To our knowledge, SPR has not been studied in any form of cancer and we provide unprecedented information on its role in NB, a deadly pediatric cancer. Our cell culture data suggest an oncogenic role for SPR; knock-down of SPR protein in NB cells greatly reduced cell proliferation. These *in vitro* studies are in agreement with *in vivo* studies which indicate that the SPR gene is a significant oncogenic factor that influences the survival probability of NB patients.

Similar to OAZ, SPR forms a heterodimeric complex with ODC but with opposing biological effects, thus suggesting an inverse and likely competitive relationship between ODC, SPR, and OAZ. Since ODC and the enzyme-dead homologue AZINs are structurally very similar, it is possible that SPR interacts with AZIN. Indeed, additional docking simulations *in silico* confirmed an SPR-AZIN interaction, with high confidence under stringent settings (data not shown). Of note, the computationally predicted interaction sites appear to be very similar to those of ODC, thus proposing a multi-component, competitive mechanism in which ODC and AZINs might compete for binding to SPR (Fig. 6c). A

detailed investigation to elucidate the underlying molecular mechanisms and multiple complex formations between ODC, SPR, OAZ, and AZIN is underway.

Interestingly, it has previously been proposed that NO inhibits ODC activity by S-nitrosylation of the ODC active site, and that in turn polyamines can inhibit the induction of NOS [38]. The newly discovered ODC-SPR interaction might contribute to this pathway cross-talk, and presents an additional level of regulation that controls both the NO and polyamine pathways.

In summary, this study introduces an entirely novel concept for the polyamine field in which two well-characterized biochemical pathways converge via the interaction and co-regulation of two enzymes, ODC and SPR. The model also proposes an oncogenic role for SPR in its direct engagement with cellular mechanisms that control ODC activity. *In vivo*, SPR has oncogenic potential in NB and possibly other forms of cancer which makes it a suitable and new molecular target for drug design and therapeutic intervention.

Materials and Methods

Protein-protein docking

The templates used for monomers, homodimers and heterocomplexes were ODC (human ornithine decarboxylase, PDB ID: 1D7K composed of two identical chains - A and B) and SPR (human sepiapterin reductase, PDB ID: 1Z6Z composed of six identical chains of which only the biological unit - chains A and B – were considered). Simulations were performed using two computation types. The first was ODA, the Optimal Docking Area method which identifies the surface elements with the most favorable (i.e. lowest) docking desolvation energies [45]. Burial of these areas upon interaction may drive the formation of protein complexes and the interaction points (ODA hot spots) may be used to support protein docking predictions. An implementation of ODA is available at http://www.molsoft.com/oda.html. The second technique was GRAMM-X, the Global Range Molecular Matching method which predicts protein-protein interaction sites based on high-resolution rigid-body geometric fit and hydrophobicity [46]. This algorithm locates the area with the minimum intermolecular energy through an exhaustive multi-dimensional search of translations and rotations between the protein pairs. GRAMM-X runs on a 320 processor Linux cluster and can be accessed at http://vakser.bioinformatics.ku.edu/resources/gramm/grammx/. To escape computation yields resulting from the order of protein input, simulations were run with every possible permutation of monomers and dimers, each chain serving as receptor and ligand in the procedure. Semi-flexible docking was performed with the original GRAMM global search algorithm on local hosts using low-resolution parameters to account for conformational changes that might occur when proteins interact with each other [59]. The predicted complexes were visualized and analyzed with the ICM-Browser (Molsoft LLC, San Diego, CA, USA).

Cell line culturing

The human NB cell line MYCN2 (provided by Jason Shohet, TX, USA) was maintained in RPMI 1640 (Mediatech, Manassas, VA, USA) containing 10% (v/v) tetracycline-free, heat-

inactivated fetal bovine serum (FBS) (Atlanta Biologicals, Lawrenceville, GA, USA). HEK293 cells were obtained from the American Type Culture Collection (Manassas, VA, USA) and maintained in DMEM (Mediatech) containing 10% (v/v) tetracycline-free, heat-inactivated fetal bovine serum (FBS) (Atlanta Biologicals, Lawrenceville, GA, USA). All cells were cultured at 37 °C, in a humidified atmosphere containing 5% CO_2.

Western blot analysis

Cell lysates were prepared in RIPA buffer (20 mM Tris-HCl, pH 7.5, 0.1% (w/v) sodium lauryl sulfate, 0.5% (w/v) sodium deoxycholate, 135 mM NaCl, 1% (v/v) Triton X-100, 10% (v/v) glycerol, 2 mM EDTA), supplemented with protease inhibitor cocktail Set V (Calbiochem, Merck Group, Darmstadt, Germany), Western blot analysis was performed as previously described [13]. The total protein concentration was determined using the Bradford-based Bio-Rad assay (Hercules, CA, USA) and quantified using a BioTek SynergyMx (Winooski, VT, USA). Cell lysates in SDS-sample buffer were incubated for 15 min at 95ºC and equal amounts of total protein analyzed by 10% SDS-polyacrylamide gel electrophoresis (SDS-PAGE) and Western blotting. The antibodies used in this study are: mouse polyclonal SPR purified MaxPab antibody B01P (Abnova, Taipei City, Taiwan) at 1:1000, affinity-purified rabbit polyclonal ODC antibody N15 (Prestige Antibodies, Sigma-Aldrich, St. Louis, MO, USA) at 1:1000 and anti-GADPH (Ambion, Invitrogen Life Technologies, Grand Island, NY, USA) at 1:10,000. IRdye 800 Secondary anti-mouse and anti-rabbit antibodies were from Licor (Lincoln, NE, USA), and secondary mouse and rabbit Alexa Fluor 680 from Invitrogen (Invitrogen Life Technologies, Grand Island, NY, USA). All secondary antibodies were used at 1:10,000. Proteins were detected using a Licor Odyssey and analyzed with Licor Image Studio 2.0 acquisition and analysis software.

Immunoprecipitation

Cells were grown to 70–80% confluence on 3 x 15 cm dishes and harvested in RIPA buffer supplemented with protease inhibitor cocktail Set V (Calbiochem). Cells were pooled and a small aliquot was taken for protein concentration determination. Equal amounts of total protein were incubated with 2 μg/ml agarose-conjugated goat polyclonal ODC or agarose-conjugated $p27^{Kip1}$ antibody (Santa Cruz Biotechnology, Santa Cruz, CA, USA) and incubated overnight at 4ºC with gentle agitation. Blocking peptide was pre-incubated for 30 minutes with agarose-conjugated antibody prior to immunoprecipitation and used in a 4:5 ratio (by weight). Agarose-protein immune complexes were washed with RIPA buffer, and proteins were eluted by adding SDS sample buffer and boiling for 10 min. The samples were briefly centrifuged to pellet agarose beads, and analyzed by SDS-PAGE and Western blot, using Licor detection as described above.

Microscopy

For immunofluorescence micrographs, cells were washed twice in PBS, fixed in 4% (w/v) paraformaldehyde in PBS for 10 min, and exposed to 0.1% (v/v) Triton X-100 in PBS for 3 min. Fixed cells were washed again, blocked in 1% (w/v) bovine serum albumin in PBS for 30 min, and incubated with rabbit polyclonal ODC antibody (H-71, sc-33539, Santa Cruz Biotechnology) at 1:50, and mouse polyclonal SPR affinity-purified MaxPab antibody (B01P (Abnova) at 1:100 over night at 4ºC. After incubation, cells were washed three times

with PBS and incubated for 1 hour with anti-rabbit Alexa Fluor 488 or anti-mouse Alexa 546 antibody at 1:2,000. DAPI was used as a nuclear stain. Coverslips were washed and mounted using ProLong Gold Antiface mounting medium (Invitrogen Life Technologies). Samples were analyzed with an inverted TSC SPE confocal microscope (Leica Microsystems, Buffalo Grove, IL, USA). Epifluorescent measurements were performed using an Operetta High Content Imaging System (PerkinElmer, Santa Clara, CA, USA) using a 96-well format.

RNAi-mediated transcript silencing

Equal amounts of cells were transfected with the NEON transfection system using 10 μl NEON electrodes according to the manufacturer's protocol (Invitrogen Life Technologies). Programs were P-I and P-II at 3 x 1200 mV for 20 ms and 2 x 1400 mV for 30 ms, respectively. Cells were transiently transfected using a pool of 3 target-specific 20–25 nt siRNAs against human SPR or ODC1, or non-targeting (scrambled) control siRNA (Santa Cruz Biotechnology). Cells were seeded in 10 cm plates containing 10 ml of RPMI or DMEM supplemented with 10% FBS and cultured as described above. Cells were harvested after 72 hours. HEK293 clones expressing anti-ODC or control shRNA were established using SureSilencing Plasmids (Qiagen, Valencia, CA, USA). Cells were selected and maintained in medium containing 100 μg/ml G418. Four HEK293 clones expressing different ODC shRNA constructs as well as two clones expressing non-targeting (scrambled) shRNA constructs were established. The clone showing the most efficient ODC knock-down was used for experiments. Equal amounts of cells were seeded and cells were harvested when the control cells reached 80–90% confluence.

Cell proliferation assays

Equal amounts of cells were transfected as described above. Cells were harvested in RIPA buffer after 72 hours. Protein concentrations were determined using the Bio-Rad assay and BioTek SynergyMx plate reader as described above. Protein concentrations were expressed as a function of the highest concentration within each individual set of experiments.

ODC enzyme activity assay

ODC enzyme activity was determined using a standard assay as previously reported [60]. In brief, cells were transfected as described above, incubated for 72 hours, washed 3 times in ice cold PBS, and harvested in ice cold buffer containing 25 mM Tris-HCl, 2.5 mM DTT, 100 μM EDTA and protease inhibitor cocktail Set V (Calbiochem). ODC activity was then measured in a reaction mixture that contained 20 μM L-[1-^{14}C]-ornithine (57.10 Ci/mol; PerkinElmer).

Affymetrix DNA micro-array hybridization and analysis

The Affymetrix NB tumor dataset Versteeg-88 contains the mRNA expression profiles of 88 NB tumors with documented genetic and clinical features, and has been described [51]. Total RNA was extracted from frozen NBs containing > 95 % tumor cells, and Affymetrix HG-U133 Plus 2.0 micro-array analysis (Affymetrix, Santa Clara, CA, USA) performed as described in [54]. The Versteeg-88 set has been deposited for public access in a MIAME-

compliant format through the Gene Expression Omnibus (GEO) database at the NCBI website [61] under number GSE16476. CEL data were analyzed as described in [54]. Briefly, gene transcript levels were determined from data image files using GeneChip operating software (MAS5.0 and GCOS1.0, from Affymetrix). Samples were scaled by setting the average intensity of the middle 96 % of all probe-set signals to a fixed value of 100 for every sample in the dataset, allowing comparisons between micro-arrays. The TranscriptView genomic analysis and visualization tool within R2 was used to check if probe-sets had an anti-sense position in an exon of the gene (http://r2.amc.nl > genome browser). The Affymetrix probe-sets selected for ODC (200790_at) and SPR (203458_at) meet these criteria and showed significant expression in 88 and 29 samples in the Versteeg-88 set, respectively. Analyses were performed using R2; a genomics analysis and visualization platform developed in the Department of Oncogenomics at the Academic Medical Center – University of Amsterdam. R2 can be accessed at: http://r2.amc.nl.

Statistical analysis

SPR correlation with survival probability was evaluated by Kaplan-Meier analysis using the Wilcoxon log-rank test as described [62]. To determine the optimal value of SPR expression to set as cut-off value, all tumor samples were first sorted according to SPR expression, and subsequently divided in two groups. For each group separation (higher or lower than the current SPR expression, minimum group size n=8), the log-rank significance was calculated. The best *P* value obtained was used to represent the final gene expression cut-off value. To correct for multiple testing, the resulting *P* value was divided by the number of tests performed (n-16, Bonferoni correction) (Kaplan Scanner in R2). ODC or SPR expression and correlation with NB clinical and genetic features were determined using the non-parametric Kruskal-Wallis test; correlation with other gene expressions was calculated with a 2log Pearson test. The significance of a correlation is determined by t = R/sqrt((1-r^2)/(n-2)), where R is the correlation value and n is the number of samples. Distribution measure is approximately as t with n-2 degrees of freedom. The statistical significance of the effects on NB cell proliferation was determined using the statistical Student's *t* test. For all tests, $P < 0.05$ was considered statistically significant.

Supplementary Material

Refer to Web version on PubMed Central for supplementary material.

Acknowledgments

We thank Dr. Dana-Lynn Koomoa for expert advice and Dr. Janos Molnar for initial contributions. Dr. Jason Shohet (Texas Children's Hospital) is thanked for providing the MYCN2 NB cell line. This work was supported by NIH grants from the National Cancer Institute R01 CA-111419 (André S. Bachmann) and R01 Supplement CA-111419-S1 (André S. Bachmann), R01 CA-018138 (David J. Feith, Anthony E. Pegg), the Dutch Cancer Society ("KWF Kankerbestrijding") UVA2005-3665 (Dirk Geerts), and the European Union COST Action BM0805 (Dirk Geerts).

References

1. Auvinen M, Jarvinen K, Hotti A, Okkeri J, Laitinen J, Janne OA, Coffino P, Bergman M, Andersson LC, Alitalo K, Holtta E. Transcriptional regulation of the ornithine decarboxylase gene by c-

Myc/Max/Mad network and retinoblastoma protein interacting with c-Myc. Int J Biochem Cell Biol. 2003; 35:496–521. [PubMed: 12565711]

2. Auvinen M, Paasinen A, Andersson LC, Holtta E. Ornithine decarboxylase activity is critical for cell transformation. Nature. 1992; 360:355–8. [PubMed: 1280331]
3. Casero RA Jr, Marton LJ. Targeting polyamine metabolism and function in cancer and other hyperproliferative diseases. Nat Rev Drug Discov. 2007; 6:373–90. [PubMed: 17464296]
4. Pegg AE, Feith DJ. Polyamines and neoplastic growth. Biochem Soc Trans. 2007; 35 :295–9. [PubMed: 17371264]
5. Nilsson JA, Keller UB, Baudino TA, Yang C, Norton S, Old JA, Nilsson LM, Neale G, Kramer DL, Porter CW, Cleveland JL. Targeting ornithine decarboxylase in Myc-induced lymphomagenesis prevents tumor formation. Cancer Cell. 2005; 7:433–44. [PubMed: 15894264]
6. Bachmann, AS.; Geerts, D.; Sholler, G. Neuroblastoma: Ornithine decarboxylase and polyamines are novel targets for therapeutic intervention. In: Hayat, MA., editor. Pediatric Cancer, Neuroblastoma: Diagnosis, Therapy, and Prognosis. Vol. 1. Springer; 2012. p. 91-103.
7. Evageliou NF, Hogarty MD. Disrupting polyamine homeostasis as a therapeutic strategy for neuroblastoma. Clin Cancer Res. 2009; 15:5956–61. [PubMed: 19789308]
8. Geerts D, Koster J, Albert D, Koomoa DL, Feith DJ, Pegg AE, Volckmann R, Caron H, Versteeg R, Bachmann AS. The polyamine metabolism genes ornithine decarboxylase and antizyme 2 predict aggressive behavior in neuroblastomas with and without MYCN amplification. Int J Cancer. 2010; 126:2012–2024. [PubMed: 19960435]
9. Hogarty MD, Norris MD, Davis K, Liu X, Evageliou NF, Hayes CS, Pawel B, Guo R, Zhao H, Sekyere E, Keating J, Thomas W, Cheng NC, Murray J, Smith J, Sutton R, Venn N, London WB, Buxton A, Gilmour SK, Marshall GM, Haber M. ODC1 Is a Critical Determinant of MYCN Oncogenesis and a Therapeutic Target in Neuroblastoma. Cancer Res. 2008; 68:9735–45. [PubMed: 19047152]
10. Koomoa DL, Geerts D, Lange I, Koster J, Pegg AE, Feith DJ, Bachmann AS. DFMO/eflornithine inhibits migration and invasion downstream of MYCN and involves p27Kip1 activity in neuroblastoma. Int J Oncol. 2013; 42:1219–1228. [PubMed: 23440295]
11. Koomoa DL, Yco LP, Borsics T, Wallick CJ, Bachmann AS. Ornithine Decarboxylase Inhibition by {alpha}-Difluoromethylornithine Activates Opposing Signaling Pathways via Phosphorylation of Both Akt/Protein Kinase B and p27Kip1 in Neuroblastoma. Cancer Res. 2008; 68:9825–31. [PubMed: 19047162]
12. Rounbehler RJ, Li W, Hall MA, Yang C, Fallahi M, Cleveland JL. Targeting ornithine decarboxylase impairs development of MYCN-amplified neuroblastoma. Cancer Res. 2009; 69:547–53. [PubMed: 19147568]
13. Wallick CJ, Gamper I, Thorne M, Feith DJ, Takasaki KY, Wilson SM, Seki JA, Pegg AE, Byus CV, Bachmann AS. Key role for p27Kip1, retinoblastoma protein Rb, and MYCN in polyamine inhibitor-induced G1 cell cycle arrest in MYCN-amplified human neuroblastoma cells. Oncogene. 2005; 24:5606–18. [PubMed: 16007177]
14. Samal K, Zhao P, Kendzicky A, Yco LP, McClung H, Gerner EW, Burns MR, Bachmann AS, Sholler G. AMXT-1501, a novel polyamine transport inhibitor, synergizes with DFMO in inhibiting neuroblastoma cell proliferation by targeting both ornithine decarboxylase and polyamine transport. Int J Cancer. 2013 In Press.
15. Bachmann AS. The role of polyamines in human cancer: prospects for drug combination therapies. Hawaii Med J. 2004; 63:371–4. [PubMed: 15704548]
16. Bachmann, AS.; Levin, VA. Clinical applications of polyamine-based therapeutics. In: Woster, PM.; Casero, RA., Jr, editors. Polyamine Drug Discovery. Royal Society of Chemistry; 2012. p. 257-276.
17. Gamble LD, Hogarty MD, Liu X, Ziegler DS, Marshall G, Norris MD, Haber M. Polyamine pathway inhibition as a novel therapeutic approach to treating neuroblastoma. Front Oncol. 2012; 2:162. [PubMed: 23181218]
18. Lu X, Pearson A, Lunec J. The MYCN oncoprotein as a drug development target. Cancer Lett. 2003; 197:125–30. [PubMed: 12880971]

19. Lutz W, Stohr M, Schurmann J, Wenzel A, Lohr A, Schwab M. Conditional expression of N-myc in human neuroblastoma cells increases expression of alpha-prothymosin and ornithine decarboxylase and accelerates progression into S-phase early after mitogenic stimulation of quiescent cells. Oncogene. 1996; 13:803–12. [PubMed: 8761302]
20. Brodeur GM. Neuroblastoma: biological insights into a clinical enigma. Nat Rev Cancer. 2003; 3:203–16. [PubMed: 12612655]
21. Maris JM. Recent advances in neuroblastoma. N Engl J Med. 2010; 362:2202–11. [PubMed: 20558371]
22. Park JR, Eggert A, Caron H. Neuroblastoma: biology, prognosis, and treatment. Hematol Oncol Clin North Am. 2010; 24:65–86. [PubMed: 20113896]
23. Matsufuji S, Matsufuji T, Miyazaki Y, Murakami Y, Atkins JF, Gesteland RF, Hayashi S. Autoregulatory frameshifting in decoding mammalian ornithine decarboxylase antizyme. Cell. 1995; 80:51–60. [PubMed: 7813017]
24. Cohavi O, Tobi D, Schreiber G. Docking of antizyme to ornithine decarboxylase and antizyme inhibitor using experimental mutant and double-mutant cycle data. J Mol Biol. 2009; 390:503–15. [PubMed: 19465028]
25. Liu YC, Hsu DH, Huang CL, Liu YL, Liu GY, Hung HC. Determinants of the differential antizyme-binding affinity of ornithine decarboxylase. PLoS One. 2011; 6:e26835. [PubMed: 22073206]
26. Liu YC, Liu YL, Su JY, Liu GY, Hung HC. Critical factors governing the difference in antizyme-binding affinities between human ornithine decarboxylase and antizyme inhibitor. PLoS One. 2011; 6:e19253. [PubMed: 21552531]
27. Su KL, Liao YF, Hung HC, Liu GY. Critical factors determining dimerization of human antizyme inhibitor. J Biol Chem. 2009; 284:26768–77. [PubMed: 19635796]
28. Pegg AE. Regulation of ornithine decarboxylase. J Biol Chem. 2006; 281:14529–32. [PubMed: 16459331]
29. Coffino P. Antizyme, a mediator of ubiquitin-independent proteasomal degradation. Biochimie. 2001; 83:319–23. [PubMed: 11295492]
30. Coffino P. Regulation of cellular polyamines by antizyme. Nat Rev Mol Cell Biol. 2001; 2:188–94. [PubMed: 11265248]
31. Mangold U. The antizyme family: polyamines and beyond. IUBMB Life. 2005; 57:671–6. [PubMed: 16223706]
32. Albeck S, Dym O, Unger T, Snapir Z, Bercovich Z, Kahana C. Crystallographic and biochemical studies revealing the structural basis for antizyme inhibitor function. Protein Sci. 2008; 17:793–802. [PubMed: 18369191]
33. Kahana C. Antizyme and antizyme inhibitor, a regulatory tango. Cell Mol Life Sci. 2009; 66:2479–88. [PubMed: 19399584]
34. Mangold U. Antizyme inhibitor: mysterious modulator of cell proliferation. Cell Mol Life Sci. 2006; 63:2095–101. [PubMed: 16847581]
35. Olsen RR, Zetter BR. Evidence of a role for antizyme and antizyme inhibitor as regulators of human cancer. Mol Cancer Res. 2011; 9:1285–93. [PubMed: 21849468]
36. Chen L, Li Y, Lin CH, Chan TH, Chow RK, Song Y, Liu M, Yuan YF, Fu L, Kong KL, Qi L, Li Y, Zhang N, Tong AH, Kwong DL, Man K, Lo CM, Lok S, Tenen DG, Guan XY. Recoding RNA editing of AZIN1 predisposes to hepatocellular carcinoma. Nat Med. 2013; 19:209–216. [PubMed: 23291631]
37. Werner ER, Blau N, Thony B. Tetrahydrobiopterin: biochemistry and pathophysiology. Biochem J. 2011; 438:397–414. [PubMed: 21867484]
38. Hillary RA, Pegg AE. Decarboxylases involved in polyamine biosynthesis and their inactivation by nitric oxide. Biochim Biophys Acta. 2003; 1647:161–6. [PubMed: 12686127]
39. Friedman J, Roze E, Abdenur JE, Chang R, Gasperini S, Saletti V, Wali GM, Eiroa H, Neville B, Felice A, Parascandalo R, Zafeiriou DI, Arrabal-Fernandez L, Dill P, Eichler FS, Echenne B, Gutierrez-Solana LG, Hoffmann GF, Hyland K, Kusmierska K, Tijssen MA, Lutz T, Mazzuca M, Penzien J, Poll-The BT, Sykut-Cegielska J, Szymanska K, Thony B, Blau N. Sepiapterin reductase

deficiency: a treatable mimic of cerebral palsy. Ann Neurol. 2012; 71:520–30. [PubMed: 22522443]

40. Sharma M, Maraganore DM, Ioannidis JPA, Riess O, Aasly JO, Annesi G, Abahuni N, Bentivoglio AR, Brice A, Van Broeckhoven C, Chartier-Harlin MC, Destée A, Djarmati A, Elbaz A, Farrer M, Ferrarese C, Gibson JM, Gispert S, Hattori N, Jasinska-Myga B, Klein C, Lesage S, Lynch T, Lichtner P, Lambert JC, Lang AE, Mellick GD, De Nigris F, Opala G, Quattrone A, Riva C, Rogaeva E, Ross OA, Satake W, Silburn PA, Theuns J, Toda T, Tomiyama H, Uitti RJ, Wirdefeldt K, Wszolek Z, Gasser T, Krüger R. Role of sepiapterin reductase gene at the PARK3 locus in Parkinson's disease. Neurobiology of Aging. 2011; 32:2108.e1–2108.e5. [PubMed: 21782285]
41. Giot L, Bader JS, Brouwer C, Chaudhuri A, Kuang B, Li Y, Hao YL, Ooi CE, Godwin B, Vitols E, Vijayadamodar G, Pochart P, Machineni H, Welsh M, Kong Y, Zerhusen B, Malcolm R, Varrone Z, Collis A, Minto M, Burgess S, McDaniel L, Stimpson E, Spriggs F, Williams J, Neurath K, Ioime N, Agee M, Voss E, Furtak K, Renzulli R, Aanensen N, Carrolla S, Bickelhaupt E, Lazovatsky Y, DaSilva A, Zhong J, Stanyon CA, Finley RL Jr, White KP, Braverman M, Jarvie T, Gold S, Leach M, Knight J, Shimkets RA, McKenna MP, Chant J, Rothberg JM. A protein interaction map of Drosophila melanogaster. Science. 2003; 302:1727–36. [PubMed: 14605208]
42. Almrud JJ, Oliveira MA, Kern AD, Grishin NV, Phillips MA, Hackert ML. Crystal structure of human ornithine decarboxylase at 2.1 A resolution: structural insights to antizyme binding. J Mol Biol. 2000; 295:7–16. [PubMed: 10623504]
43. Auerbach G, Herrmann A, Gutlich M, Fischer M, Jacob U, Bacher A, Huber R. The 1.25 A crystal structure of sepiapterin reductase reveals its binding mode to pterins and brain neurotransmitters. EMBO J. 1997; 16:7219–30. [PubMed: 9405351]
44. Kern AD, Oliveira MA, Coffino P, Hackert ML. Structure of mammalian ornithine decarboxylase at 1.6 A resolution: stereochemical implications of PLP-dependent amino acid decarboxylases. Structure. 1999; 7:567–81. [PubMed: 10378276]
45. Fernandez-Recio J, Totrov M, Skorodumov C, Abagyan R. Optimal docking area: a new method for predicting protein-protein interaction sites. Proteins. 2005; 58:134–43. [PubMed: 15495260]
46. Tovchigrechko A, Vakser IA. GRAMM-X public web server for protein- protein docking. Nucleic Acids Res. 2006; 34:W310–4. [PubMed: 16845016]
47. Lopez-Contreras AJ, Sanchez-Laorden BL, Ramos-Molina B, de la Morena ME, Cremades A, Penafiel R. Subcellular localization of antizyme inhibitor 2 in mammalian cells: Influence of intrinsic sequences and interaction with antizymes. Journal of cellular biochemistry. 2009; 107:732–40. [PubMed: 19449338]
48. Pegg AE. Regulation of ornithine decarboxylase. The Journal of biological chemistry. 2006; 281:14529–32. [PubMed: 16459331]
49. Koomoa DL, Borsics T, Feith DJ, Coleman CC, Wallick CJ, Gamper I, Pegg AE, Bachmann AS. Inhibition of S-adenosylmethionine decarboxylase by inhibitor SAM486A connects polyamine metabolism with p53-Mdm2-Akt/protein kinase B regulation and apoptosis in neuroblastoma. Mol Cancer Ther. 2009; 8:2067–75. [PubMed: 19584241]
50. Koomoa DL, Go RC, Wester K, Bachmann AS. Expression profile of PRAF2 in the human brain and enrichment in synaptic vesicles. Neurosci Lett. 2008; 436:171–6. [PubMed: 18395978]
51. Fardin P, Barla A, Mosci S, Rosasco L, Verri A, Versteeg R, Caron HN, Molenaar JJ, Ora I, Eva A, Puppo M, Varesio L. A biology-driven approach identifies the hypoxia gene signature as a predictor of the outcome of neuroblastoma patients. Mol Cancer. 2010; 9:185. [PubMed: 20624283]
52. Gawecka JE, Geerts D, Koster J, Caliva MJ, Sulzmaier FJ, Opoku-Ansah J, Wada RK, Bachmann AS, Ramos JW. PEA15 impairs cell migration and correlates with clinical features predicting good prognosis in neuroblastoma. Int J Cancer. 2012; 131:1556–68. [PubMed: 22213050]
53. Geerts D, Wallick CJ, Koomoa DL, Koster J, Versteeg R, Go RC, Bachmann AS. Expression of prenylated Rab acceptor 1 domain family, member 2 (PRAF2) in neuroblastoma: correlation with clinical features, cellular localization, and cerulenin-mediated apoptosis regulation. Clin Cancer Res. 2007; 13:6312–9. [PubMed: 17975142]
54. Revet I, Huizenga G, Chan A, Koster J, Volckmann R, van Sluis P, Ora I, Versteeg R, Geerts D. The MSX1 homeobox transcription factor is a downstream target of PHOX2B and activates the Delta-Notch pathway in neuroblastoma. Exp Cell Res. 2008; 314:707–19. [PubMed: 18201699]

55. Gerner EW, Meyskens FL Jr. Polyamines and cancer: old molecules, new understanding. Nat Rev Cancer. 2004; 4:781–92. [PubMed: 15510159]

56. Sholler, G.; Gerner, E.; Bergendahl, G.; LaFleur, BJ.; VanderWerff, A.; Ashilkaga, T.; Ferguson, W.; Roberts, W.; Wada, RK.; Eslin, D.; Kraveka, J.; Kaplan, J.; Mitchell, D.; Parikh, NS.; Neville, K.; Sender, L.; Higgins, T.; Kawakita, M.; Hiramatsu, K.; Moriya, SS.; Bachmann, AS. A phase I trial of DFMO as a single agent and in combination with etoposide in patients with refractory or recurrent neuroblastoma. Annual Meeting of the American Association for Cancer Research (AACR); Washington, D.C. 2013. p. LB-179.

57. Lohmann E, Koroglu C, Hanagasi HA, Dursun B, Tasan E, Tolun A. A homozygous frameshift mutation of sepiapterin reductase gene causing parkinsonism with onset in childhood. Parkinsonism Relat Disord. 2012; 18:191–3. [PubMed: 22018912]

58. Lewandowski NM, Ju S, Verbitsky M, Ross B, Geddie ML, Rockenstein E, Adame A, Muhammad A, Vonsattel JP, Ringe D, Cote L, Lindquist S, Masliah E, Petsko GA, Marder K, Clark LN, Small SA. Polyamine pathway contributes to the pathogenesis of Parkinson disease. Proc Natl Acad Sci U S A. 2010; 107:16970–5. [PubMed: 20837543]

59. Katchalski-Katzir E, Shariv I, Eisenstein M, Friesem AA, Aflalo C, Vakser IA. Molecular surface recognition: determination of geometric fit between proteins and their ligands by correlation techniques. Proc Natl Acad Sci U S A. 1992; 89:2195–9. [PubMed: 1549581]

60. Coleman CS, Pegg AE. Assay of mammalian ornithine decarboxylase activity using [14C]ornithine. Methods Mol Biol. 1998; 79:41–4. [PubMed: 9463815]

61. Barrett T, Troup DB, Wilhite SE, Ledoux P, Rudnev D, Evangelista C, Kim IF, Soboleva A, Tomashevsky M, Marshall KA, Phillippy KH, Sherman PM, Muertter RN, Edgar R. NCBI GEO: archive for high-throughput functional genomic data. Nucleic Acids Res. 2009; 37:D885–90. [PubMed: 18940857]

62. Bewick V, Cheek L, Ball J. Statistics review 12: survival analysis. Crit Care. 2004; 8 :389–94. [PubMed: 15469602]

Highlights

- New paradigm for pathway interaction by protein-protein binding of sentinel pathway enzymes ornithine decarboxylase (ODC) and sepiapterin reductase (SPR) discovered.
- Molecular modeling predicts both monomer and dimer interaction between ODC and SPR, *in silico*.
- Native enzymes ODC and SPR interact at physiological levels, *in vivo*.
- SPR suppression reduces ODC enzyme activity and suppresses neuroblastoma cell proliferation.

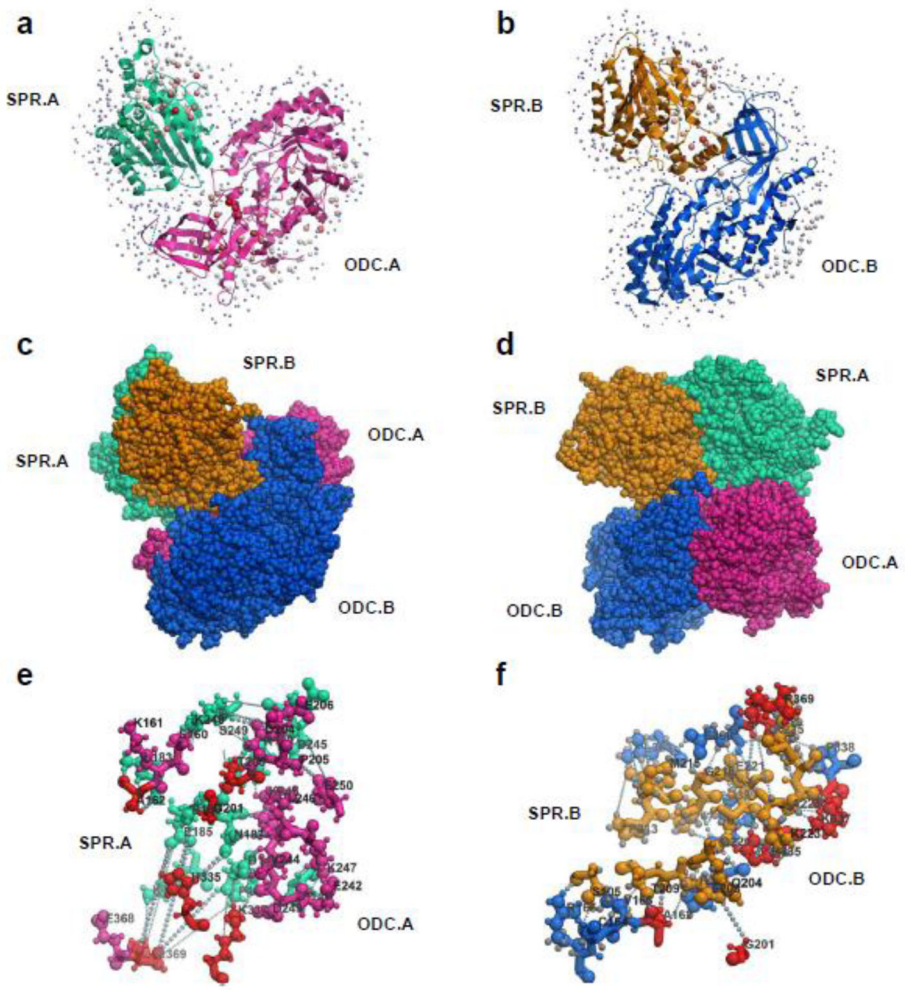

Fig. 1.

Docking simulation of SPR (1Z6Z) with ODC (1D7K). Computations were performed using GRAMM-X and ODA methodologies and the resulting structures were analyzed with the ICM-Browser (see Materials and Methods). (a) Docking of individual monomeric components SPR.A and ODC.A – a view set to the orientation of ODC.A chain as defined in the PDB file. Chains are illustrated as ribbons and colored individually: ODC.A (magenta) and SPR.A (green). ODA hot spots (optimal docking areas) are shown as colored spheres (blue to red), ranked according to the desolvation energies of the surface elements. (b) Docking of monomeric components SPR.B (orange) and ODC.B (blue) shown from the same perspective as in (a) but the projection differs by a 180 degree rotation to reflect the orientation of these chains in the dimer. (c) Docking of symmetric homodimers. The protein complex is illustrated as a space fill view and colored as above. The orientations of the chains are the same as in (a) and (b). (d) Same as (c) except with the protein complex rotated left and top-down to show the dimer-dimer interface and the tightly packed quaternary structure of the four components. (e) A close-up view of the intermolecular surface between SPR.A and ODC.A from (a) and (c). The complex is oriented to highlight the binding site. Residue-to-residue contacts (ranging from 1 Å to 7 Å) are shown as lines of gray balls. (f) Structure of the SPR.B/ODC.B binding site from (b) and (d). Residues common to both binding modes are colored red in (e) and (f). Owing to the symmetric nature of the two homodimers, docking with opposite polarity results in indistinguishable configurations from those shown in the figure. While A chain to A chain assemblies serve here as selected examples, flipped A-chain to B-chain interfaces could be equally presented.

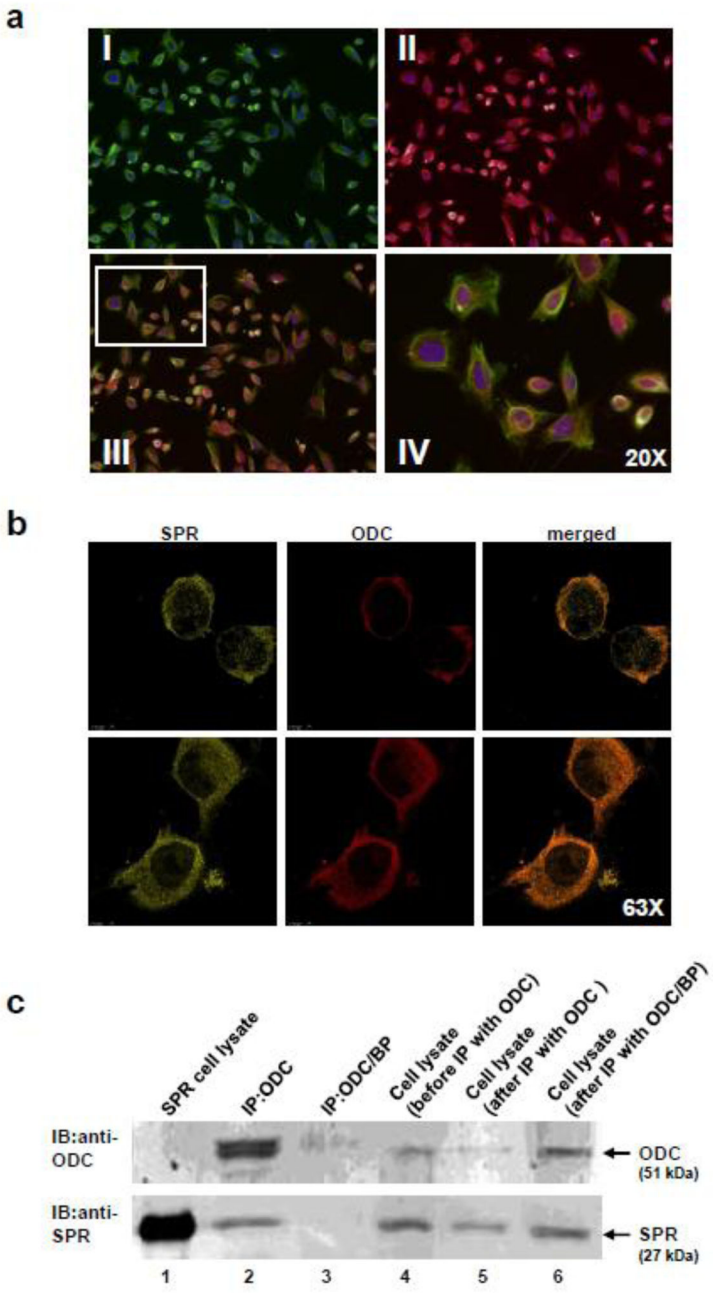

Fig. 2.

Co-localization and co-immunoprecipitation of ODC and SPR in NB cells. (a) Detection of ODC and SPR cellular localization by immunofluorescence. Epifluorescent images were acquired using the Operetta High-Content Imaging System. DAPI (blue) was used as a nuclear counter stain. Panels I-IV show 20X magnification of NB cells stained with polyclonal antibodies specific for human ODC (red) and human SPR (green). Panel III shows a superposition of panels I and II. Panel IV is a power image of panel III to better visualize the stained sub-cellular structures. (b) Images of representative cells detected in two independent experiments (top/bottom panels). Individual channels as well as a superposition of SPR and ODC are shown using confocal microscopy at 63X magnification. Endogenous ODC (red) and endogenous SPR (green) co-localize as shown in the merged images (yellow). (c) Endogenous ODC was immunoprecipitated from lysates of MYCN2 NB cells using agarose-conjugated

goat polyclonal antibody targeting ODC. The resulting protein precipitates were separated using SDS-PAGE and endogenous enzymes ODC and SPR were detected using Western blot analysis. In lane 1, a commercially available SPR lysate (from HEK293 cells) with over-expressed SPR was included as control showing the SPR-specific band at a predicted Mw of 27 kDa. In lane 2, ODC co-immunoprecipitated SPR in cell lysate from MYCN2 cells and the precipitation was suppressed when an ODC antibody-specific blocking peptide (BP) was included with the ODC immunoprecipitation reaction (Lane 3). Lane 4 shows detection of ODC and SPR in cell lysates, before ODC immunoprecipitation. Lanes 5 and 6 show detection of ODC and SPR from cell lysates of lanes 2 and 3, after ODC immunoprecipitation. BP, blocking peptide; IB, immunoblot; IP, immunoprecipitation.

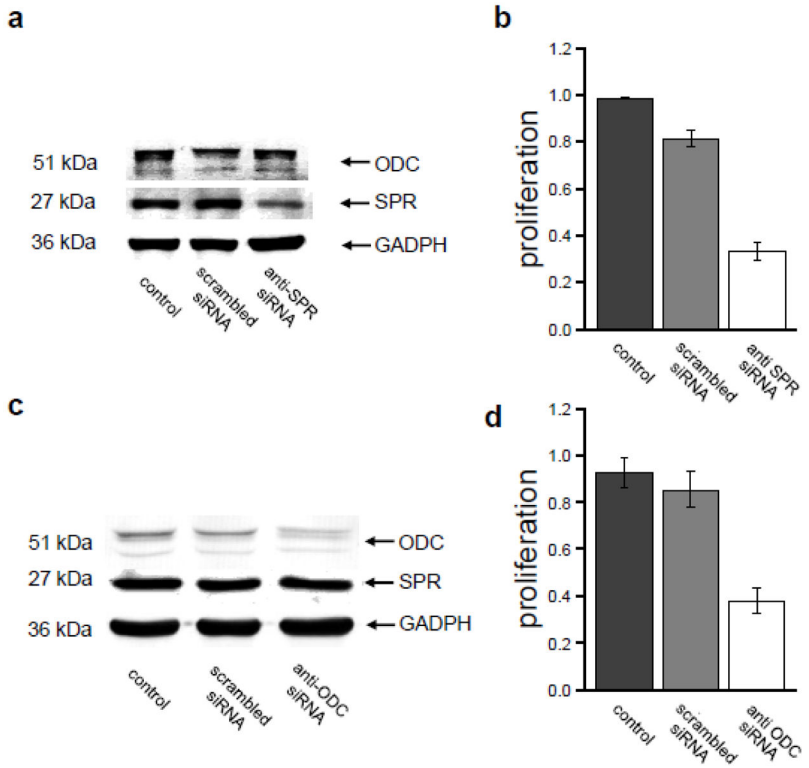

Fig. 3.

Knock-down of SPR and ODC by siRNA inhibits cell proliferation in NB cells. (a) SPR was down-regulated in NB cells using siRNA. Control cells were either exposed to non-targeting scrambled siRNA or in the absence of siRNA. Total protein cell lysates were subjected to SDS-PAGE and Western blot analysis, using antibodies specific for ODC, SPR, and GAPDH (loading control). The knock-down of SPR by siRNA did not affect ODC or GADPH levels. (b) Equal amounts of cells were seeded and protein levels were compared after 72 hours (n=10). Proliferation was significantly reduced in cells that were treated with siRNA targeting SPR. (c) ODC was down-regulated in NB cells using siRNA. Control cells were either exposed to non-targeting scrambled siRNA or in the absence of siRNA. Total protein was isolated and subjected to SDS-PAGE and Western blot analysis as described in (a). The knock-down of ODC did not affect SPR or GADPH levels. (d) equal amounts of cells were seeded and protein levels of the three different conditions were compared 72 hours later (n=3). As observed for SPR (b), proliferation was significantly reduced in cells that were treated with ODC-targeting siRNA.

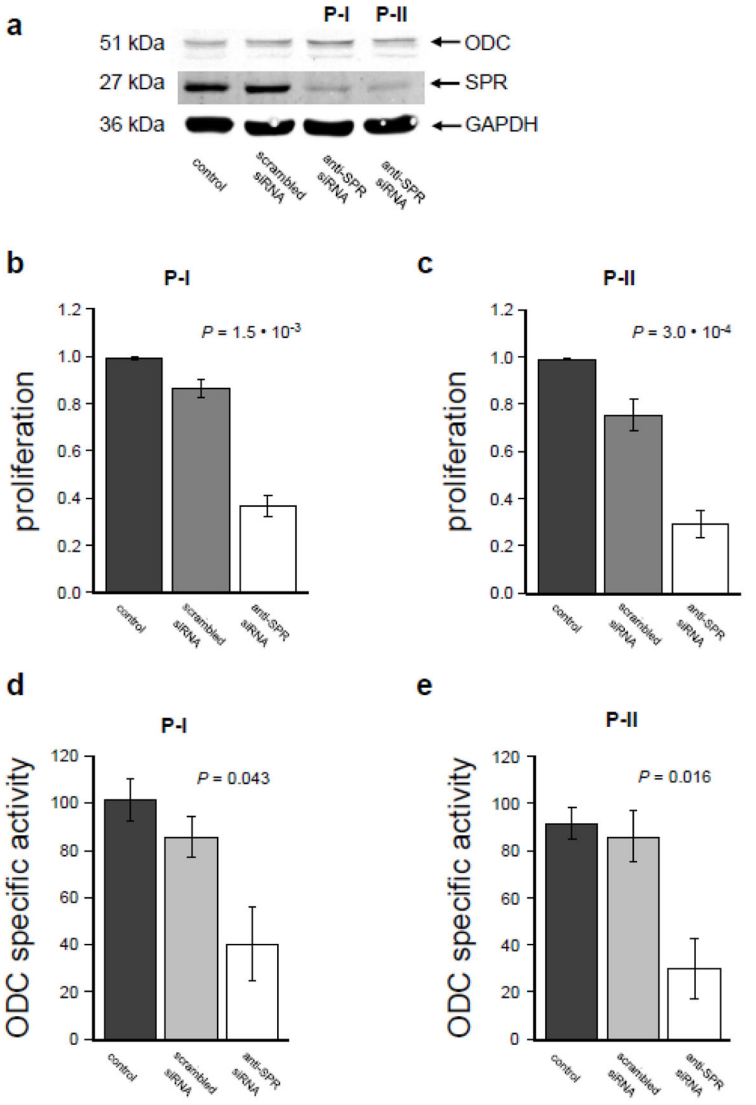

Fig. 4.

SPR protein expression regulates ODC enzymatic activity and cellular proliferation in NB cells. (a) MYCN2 cells were treated with siRNA against SPR using two different transfection protocols, referred to as protocols P-I and P-II, which differ in their voltage settings. Control cells were either transfected with non-targeting scrambled siRNA or mock transfected in the absence of siRNA. P-II was more efficient in SPR knock-down than P-I. Cell lysates were prepared and subjected to SDS-PAGE and Western blot analysis using antibodies specific for ODC, SPR, and GAPDH (loading control). Knock-down of SPR using P-II showed greater reduction of SPR levels than with P-I. (b, c) Equal amounts of cells were seeded and total amount of protein compared 72 hours later using the P-I (b) and P-II (c) transfection protocols (n=4 each). The cellular proliferation was significantly reduced by SPR siRNA in both experimental settings, and a greater anti-proliferative effect was achieved by the stronger knockdown of SPR using the P-II protocol (d, e). ODC enzymatic activity was determined in NB cells in which SPR was down-regulated using transfection protocols P-I and P-II and compared to cells treated with non-targeting scrambled siRNA or mock transfected cells in the absence of siRNA. Specific enzymatic activities are expressed as pmol CO_2/30 min/mg protein. Each sample was measured in triplicates and represents the mean of four independent experiments (n=4). The ODC enzymatic

activity was significantly reduced in both sets where SPR was down regulated using siRNA (protocol P-I; $P = 0.043$ and protocol P-II; $P = 0.016$).

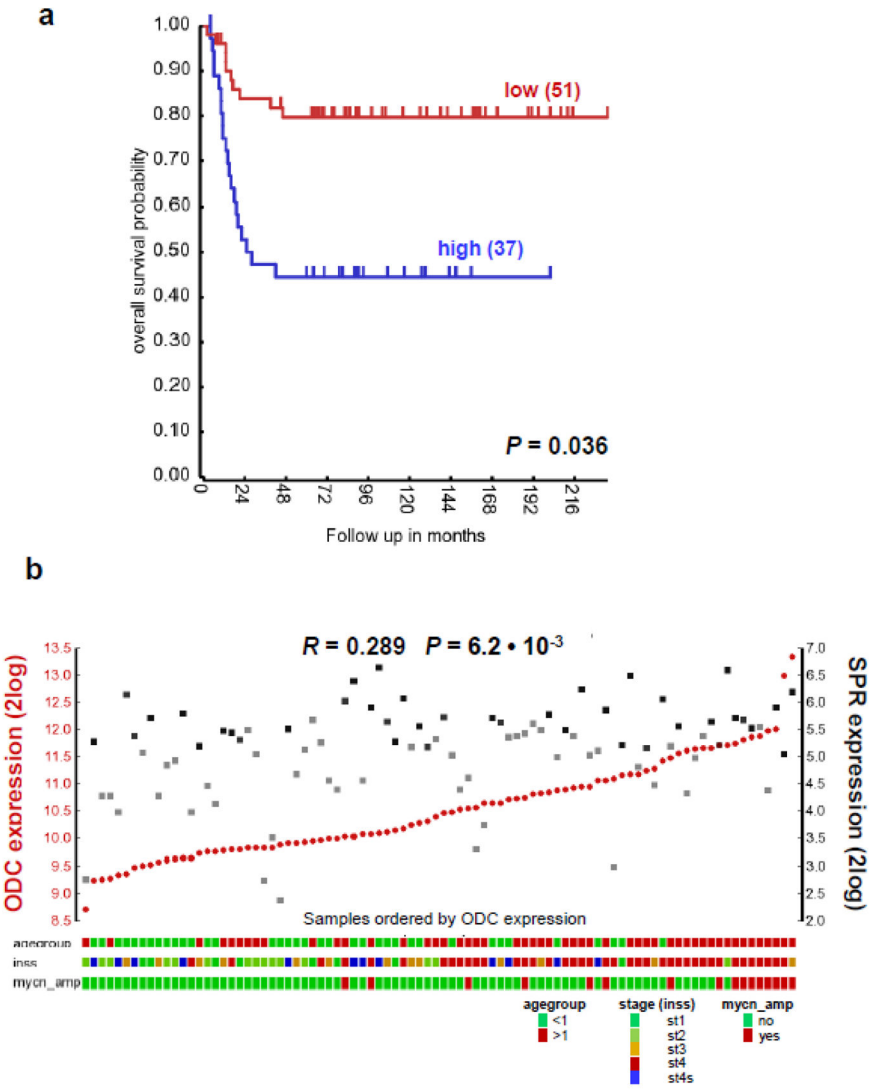

Fig. 5.

Correlation of SPR gene expression with NB patient prognosis and ODC gene expression. (a) Prognostic significance of SPR expression in NB. Kaplan-Meier graph representing the survival prognosis of 88 NB patients based on high or low expression of SPR in their tumor. The survival probability of NB patients (follow-up over 216 months) with low SPR tumor expression is significantly higher than of patients with high SPR tumor expression. The most significant *P* value obtained by repeated grouping (see Materials and Methods) was $P = 0.036$ after stringent Bonferoni correction. This grouping separated 37 patients with high tumor SPR expression and a survival of ~45% from 51 patients with low tumor SPR expression and a survival of ~80%. This prognostic significance was also found for other groupings: for median SPR expression cut-off (grouping 44 tumors with high against 44 with low SPR expression) and for average SPR expression cut-off (grouping 41 tumors with high, against 47 with low SPR expression), the *P* values were 0.024 and $5.8 \cdot 10^{-3}$, respectively. (b) ODC and SPR expression correlation in NB tumors: visual representation of ODC and SPR expression in all 88 NB samples, ranked horizontally from left to right according to their ODC expression. ODC and SPR expression values for each tumor are visualized with red circles and black rectangles, respectively. The correlation between ODC and SPR expression is r = 0.289, with a *P* value of $6.2 \cdot 10^{-3}$ (2logPearson). Below the graph are the symbols representing the clinical values of the tumor samples, with their legend.

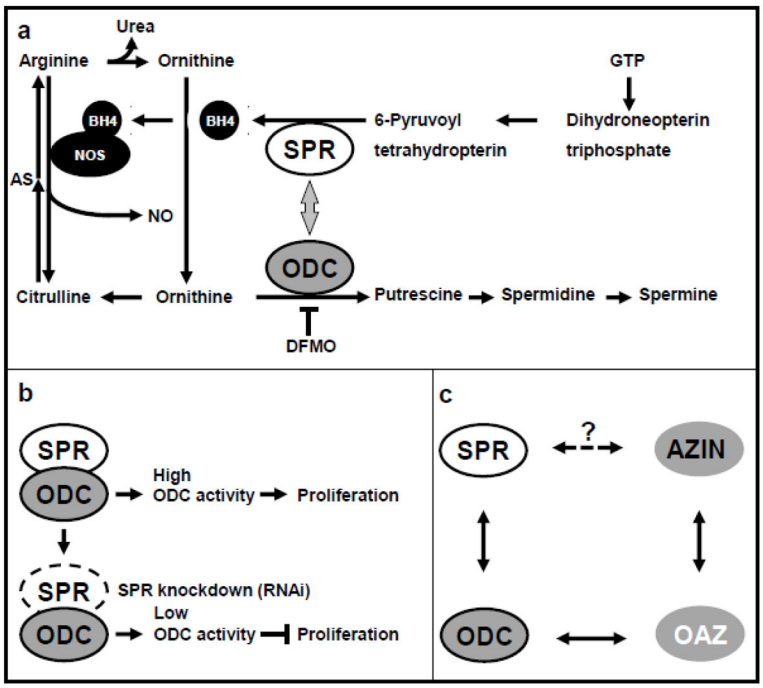

Fig. 6.

Proposed crosstalk between polyamine and nitric oxid (NO) pathways and schematic presentation of ornithine decarboxylase (ODC) interaction partners. (a) Arginine is converted to ornithine by the action of arginase in the urea cycle. The enzyme ODC converts ornithine to putrescine and is a key enzyme in the biosynthesis of higher polyamines (spermidine, spermine). The NO pathway enzyme sepiapterin reductase (SPR) converts 6-pyruvoyl tetrahydropterin to tetrahydrobiopterin (BH_4), a cofactor for NO synthase (NOS) which converts arginine to citrulline. In reverse, citrulline converts to arginine via argininosuccinate (AS) (b) ODC forms a heterodimer complex with SPR which activates ODC and stimulates cell proliferation. Downregulation of SPR in neuroblastoma (NB) cells leads to significant inhibition of ODC activity and reduces cell proliferation. The biological unit for both ODC and SPR proteins is a homodimer (in graphic depicted as an oval). (c) Antizymes (OAZs) are well known to interact with ODC and bind with greater affinity to antizyme inhibitors (AZINs). In this study, a novel concept for the field of polyamines is introduced in which SPR interacts with ODC and presents another means to control ODC activity, by potentially out-competing OAZ. Based on computational docking predictions, it is also possible that SPR interacts with AZIN, but the functional consequence of this association remains to be determined. Our discovery promises new inroads for target intervention and manipulation of the polyamine pathway which, given the recent explosion of clinical trials with DFMO in chemoprevention studies, is both timely and important.